

HARDNESS AND TRIBOLOGICAL BEHAVIOR OF CRAB SHELL PARTICLES REINFORCED ALUMINUM 6063 COMPOSITES

Adebayo Felix Owa^{1,2}, Takalani Madzivhandila¹, Peter Apata Olubambi¹,
Hammed Amokun², Ogunje Walter²

¹Centre of Nanoengineering and Advanced Materials

Department of Metallurgy, Faculty of Engineering and Built Environment

University of Johannesburg, Johannesburg 2092

South Africa, adebayowa@gmail.com (A.F.O.); tmadzivhandila@uj.ac.za (T.M.);

polubambi@uj.ac.za (P.A.O.);

²Department of Materials and Metallurgical Engineering

Faculty of Engineering, Federal University Oye-Ekiti

Ekiti State 370111, Nigeria, amokun1037@fuoye.edu.ng (H.M.);

ogunje1026@fuoye.edu.ng (O.W.)

Received 27 May 2025

Accepted 05 January 2026

DOI: 10.59957/jctm.v61.i2.2026.14

ABSTRACT

The hardness and tribological behaviour of crab shell particles (CSPs) reinforced aluminium 6063 (Al-Mg-Si alloy) composites produced by the double stir casting method were investigated. Adding CSPs caused a marked improvement in the hardness and fracture toughness of the CSP composites, reflecting enhanced fracture resistance. The wear resistance enhancement of 1.56 % was noticed in 20 wt. % CSP composite, and abrasive wear was confirmed as the main wear process for the composites. The CSP composites showed a slight reduction in the density; with very low porosity indicating satisfactory wettability for the aluminium matrix, thus making the produced composite a good candidate material for the area of engineering lightweight applications.

Keywords: wear resistance; CSPs; hardness; density; composites; aluminium 6063.

INTRODUCTION

Researchers are still working on aluminium matrix composites (AMCs) due to their success in various applications in the engineering field [1, 2], despite the extensive literature on the subject. The utility of AMC is attributed to the appealing variety of properties of composite systems, due to its adaptability to both fiber and particulate reinforcements [3, 4]. Arendarchuck et al investigated the hardness and wear resistance of NbC-reinforced A380 aluminium alloys. They concluded that the composite was more wear-resistant and hardened, especially the samples containing 15 % NbC [5]. The wear properties of AA7075 were studied; the alloy showed enhancement in wear resistance and they found that oxidation, and delamination are the mechanisms in

all the samples [6]. Silicon carbide and palm kernel shell particles were utilized to reinforce 6063 aluminium and wear experiments were carried out on the composites. They found that the density and percentage porosity of the metal matrix composite cast at 2 to 2.4 % was within the acceptable range of less than 4 %, and the composites' wear resistance was not enhanced [7]. Tribological properties of aluminium hypereutectic alloy (A390) reinforced with Ti₂AlC was studied, Ti₂AlC particles improve the wear behaviour of A390 alloy, and they opined further that an abrasive wear mechanism was observed [8].

Al6063-silicon nitride metal matrix composite was manufactured according to the process of agitation casting in liquid metallurgy technology and wear resistance improvement was reported [9]. The high-

frequency friction rig (HFRR) was used to study Al-Cu-Cr alloy, and better corrosion and wear resistance associated with microstructure improvements were reported [10]. The investigation of tribological behaviour of Okaba coal ash (OCA) reinforced Al 6063 alloy was studied and the authors opined that in comparison to base metals, all composite products recorded an increase in wear behaviour [11].

EXPERIMENTAL

Materials and method

Al-Mg-Si alloy was sourced locally, the alloy contains 1.39 wt. % Mg, 3.55 wt. % Si, 1.12 wt. % Ca, 0.79 wt. % Cl, 0.09 wt. % Cr, 0.09 wt. % V, 0.09 wt. % Ti, 0.29 wt. % Zn, 0.34 wt. % Cu, 0.33 wt. % Fe, 0.34 wt. % Mn, 0.19 wt. % Ta and 91.39 wt. % Al. The CS particle size used to produce the composites ranges from 40 to 60 μm as reported in previous studies [12]. Fig. 1 shows the flow diagram adopted in the particles production.

Composite development

All the composite samples were cast via double stir sand casting technique [13]. The Al-Mg-Si alloy was melted in a gas fired crucible within the temperature of 750 - 810°C. The melt was stirred for 120 s before casting the control at temperature of 750°C. Other samples were produced at 5, 10, 15 and 20 weight percentages of particles (40 - 60 μm) in Al-Mg-Si alloy matrix and the melt were stirred for 600 s at speed of 350 - 450 rpm.

The composite nomenclature is as follows:

- Control sample contains 100 wt. % Al-Mg-Si alloy
- 5 wt. % sample contains 5 wt. % CSPs and 95 wt. % Al-Mg-Si alloy
- 10 wt. % sample contains 10 wt. % CSPs and 90

wt. % Al-Mg-Si alloy

15 wt. % sample contains 15 wt. % CSPs and 85 wt. % Al-Mg-Si alloy

20 wt. % sample contains 20 wt. % CSPs and 80 wt. % Al-Mg-Si alloy

Determination of percentage porosity and density

The weight (measured with a digital weighing balance) was used to divide the volume for samples' density determination. Eq. (1) was adopted in determining the CSP composite theoretical density [14].

$$\rho_{\text{com}} = \text{wt}_{\text{Al6063}} \times \rho_{\text{Al6063}} + \text{wt}_{\text{CSPs}} \times \rho_{\text{CSPs}} \quad (1)$$

where ρ_{com} is the composite density, $\text{wt}_{\text{Al6063}}$ is Al 6063 weight fraction, ρ_{Al6063} is Al 6063 density, wt_{CSPs} is CSPs weight fraction, ρ_{CSPs} is CSPs density.

The composite porosity percentage was calculated by adopting Eq. (2), as determined by Alaneme and Aluko [14].

$$\% \text{ porosity} = \frac{\rho_T - \rho_{EX}}{\rho_T} \quad (2)$$

where; ρ_T is Theoretical Density, ρ_{EX} is Experimental Density.

CSP composite hardness measurement

ASTM E-92 standard was followed in the preparation and testing of the hardness samples [15]. The specimens were polished and underwent 5 indentations for 15 s each with a load of 10 N until a permanent indentation was achieved. Indentation average reading was recorded.

CSP composite fracture toughness (K_{IC})

The CSP composite fracture toughness was determined by adopting the Circumferential Notch

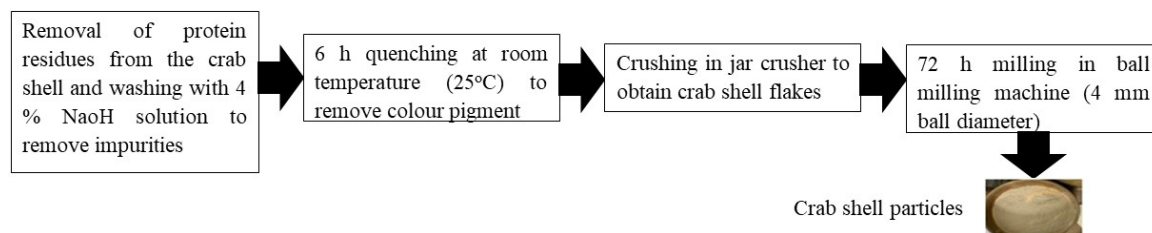


Fig. 1. Particle production route.

Tensile (CNT) testing technique, the specimen dimensions are as stated: Diameter (D) is 6 mm, 4.5 mm is the notch diameter (d), 30 mm is the gauge length, and 60° is the notch angle [14, 16].

The tensile loading to fracture of the samples was performed on an Instron universal testing machine, operated at 10^{-3} s^{-1} strain rate, and the specimens used for the fracture toughness determination are shown in Fig. 2.

Eq. (3) was adopted to calculate the composite fracture toughness (K_{ic}) [17].

$$K_{ic} = \frac{P_f}{D^{3/2}} \left[1.72 \left(\frac{D}{d} \right) - 1.27 \right] \quad (3)$$

where Fracture load is P_f , Sample diameter is D and Notch diameter is d.

Eq. (4) was used to evaluate plane strain conditions to validate the results of the composite fracture toughness.

$$D \geq \left(\frac{K_{ic}}{\sigma_y} \right)^2 \quad (4)$$

Also, during the production of the CNT test specimen, the condition that at least 4D must be equal to the length of the specimen was taken into consideration.

CSP composite wear behaviour

The wear behaviour of the samples of dimensions (200 mm diameter and 6 mm thickness), was done using the Taber abrasion wear index measurement at a speed of 500 rpm and the worn abrasion test samples surfaces were examined with SEM machine. Eq. (5) was used to evaluate the wear index of the samples, as stated by Dieter [18]:

$$\text{Wear Index (W.I)} = \frac{\text{Initial weight} - \text{Final weight}}{\text{Time of test Cycle}} \times 100\%$$

where the weights are in grams, and the time in minutes.

The morphology of the worn surfaces' samples was examined following standard protocol [13].-

RESULTS AND DISCUSSION

The representative morphology showing the EDX spectra of the composites is shown in Fig. 3. It is evident that the particle displays an irregular shape. As noted in

the EDX, the high concentration of Oxygen (60.91 wt Conc) and Calcium (30.62 wt Conc) is an indication that calcium carbonate (CaCO_3) is dominant phase in crab shell particles. Also noted is the concentration of Fe (5.45 wt Conc) introduced by the attrition effect of the milling balls.

CSP composite percentage porosity and density

Table 1 presents the density and percentage porosity of the CSP composites produced. It was observed that the density of the composites varies inversely proportional to the wt. % of CSP content. This is anticipated because 2.7 g cm^{-3} aluminium density is higher than 1.3 g cm^{-3} CSP density. All the composites have a percentage of porosity below 2.4 %, a value which is well below the permissible 4 % for matrix composite, and this strongly indicates that the double-stir casting method is effective [19]. The results also suggest that CSPs have a satisfactory wettability for aluminium, and otherwise, the porosity percentage would have been higher.

CSP composite fracture toughness

Fig. 4 presents the results of the fracture toughness of the composites; a marked fracture toughness enhancement was observed for all the composites as the wt. % CSPs content increased. The highest improvement of 47.90 % was observed in 20 % CSP composite fracture toughness ($1.821 \text{ MPa}\sqrt{m}$); while the least of 28.19 % fracture toughness ($1.578 \text{ MPa}\sqrt{m}$) was observed in 15 %

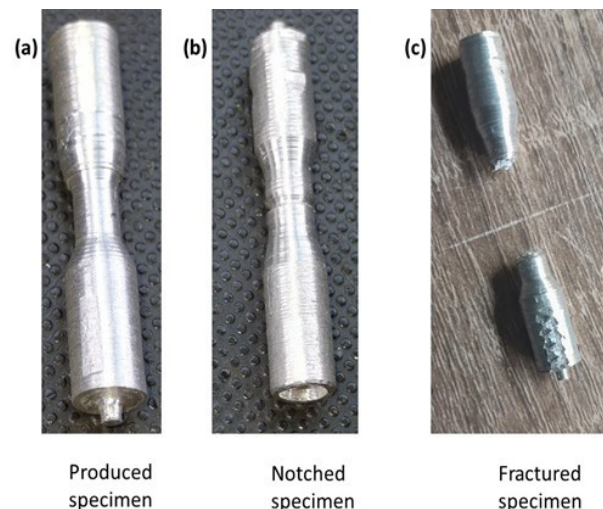


Fig. 2. Produced specimen (a), Notched specimen (b), and Fractured specimen (c).

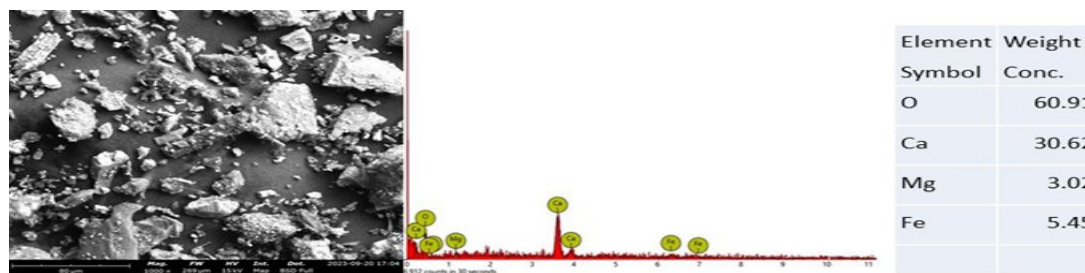


Fig. 3. SEM image and EDS pattern of CSPs.

Table 1. Composite percentage porosity and density.

SN	Sample Designation	Theoretical Density, g cm ⁻³	Experimental Density, g cm ⁻³	Porosity, %
1	Neat	2.70		
2	5 % CSPs Composite	2.635	2.5981	1.024
3	10 % CSPs Composite	2.560	2.5275	1.270
4	15 % CSPs Composite	2.475	2.4290	1.859
5	20 % CSPs Composite	2.420	2.3931	1.111

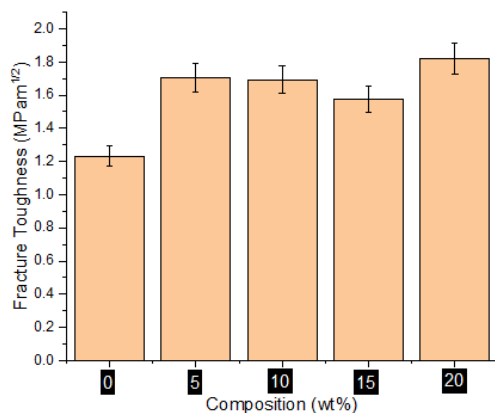


Fig. 4. Fracture toughness of the Neat and CSP-composites.

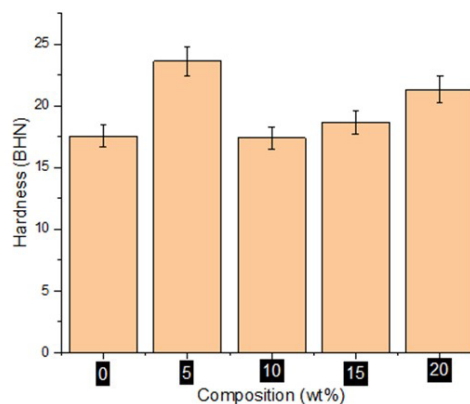


Fig. 5. Hardness of the neat and CSP composites.

CSP composite compared with the neat (1.231 MPa√m). The improvement may be attributed to the percentage porosity of less than 2.4 % of the composites as shown in Table 3, due to the double stir casting method's efficiency. The effect of particulate-matrix interfacial adhesion on the mechanical behaviour of particulate-filled composite is markedly reported in the literature [20, 21].

CSP composite hardness

Fig. 5 shows the CSP composites hardness results, the hardness of the CSP composites increased in a non-linear way as the percentage compositions of the

CSPs increased. 5 % CSP-composite recorded the highest enhancement of about 35.69 % (23.61 BHN), while 10 % CSP-composites recorded the least enhancement of 0.92 % (17.56 BHN) compared with the neat (17.40 BHN). The development is partly attributed to the percentage porosity of less than 2.4 % of the composites and the homogeneity of the composite constituents because of double stir casting technique adopted; which improved load transfer and stress distribution within the composite.

CSP composite wear behaviour

The wear resistance of the neat and CSP composites

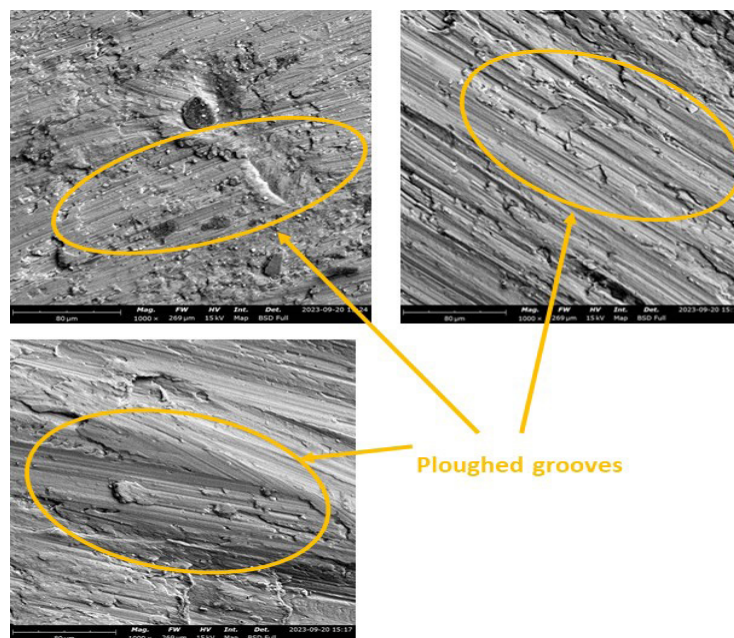


Fig. 6. Wear resistance of the Neat and CSP composites.

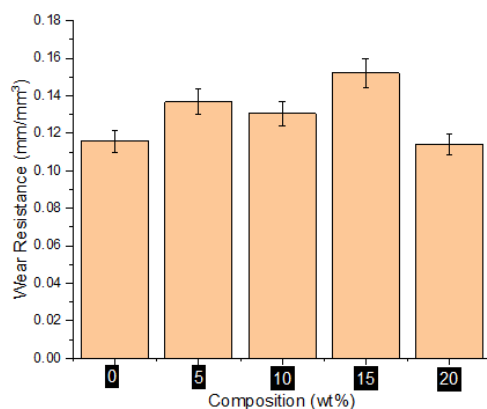


Fig. 7. SEM of representative of worn surfaces of CSP composite.

(Figs. 6 and 7) shows the representative of the SEM images of the worn surfaces of the composites. It is observed that only 20 wt. % composite has an enhancement of 1.56 % in wear resistance ($0.1140 \text{ mm mm}^{-3}$) compared with the neat ($0.1158 \text{ mm mm}^{-3}$). The lowed grooves shown in the wear tracks (Fig. 7), are revealing of the wear mechanism to be abrasive [22 - 24].

CONCLUSIONS

Crab shell particles reinforced aluminium 6063 composites were produced via the double stir casting technique, the composite hardness and tribological

behaviour were investigated. The findings are as stated:

- Milling of crab shells for 72 h in ball mills produced crab shell particles of sizes 40-50 μm and the CSPs main constituents are oxygen and calcium; combined in the form of CaCO_3 .
- The addition of CSPs slightly reduced the density, while the percentage porosity was lower than the permissible value in the composites, indicating good wettability for the aluminium matrix, thus making the produced composite a good candidate material for the area of lightweight applications.
- All the CSP composites have an enhancement in fracture toughness, indicating fracture resistance enhancement.
- The hardness of the composites was enhanced not linearly, as the CSPs wt. % increases. Only 20 % CSP composite had 1.56 % wear resistance enhancement, and the wear mechanism of the composites is abrasive.

Acknowledgments

This work was funded by the Tertiary education trust fund (TETFund) of Nigeria. It is a pleasure to thank the Centre of Nanoengineering and Tribocorrosion, University of Johannesburg, South Africa for providing the laboratory facilities for this research.

Authors' contributions

A.F.: conceptualization, formal analysis, funding acquisition, investigation, methodology, writing - original draft; H.A.: investigation, methodology, writing - original draft; W.O.: investigation, methodology, writing - original draft; T.M.: investigation, review and editing; P.A.: supervision, review and editing

REFERENCES

1. D.K. Koli, G. Agnihotri, R. Purohit, Advanced aluminium matrix composites: the critical need of automotive and aerospace engineering fields, *Mater. Today: Proc.*, 2, 2015, 3032-3041.
2. J. Singh, A. Chauhan, Characterization of hybrid aluminium matrix composites for advanced applications - a review, *J. Mater. Res. Technol.*, 5, 2016, 159-169.
3. K.K. Alaneme, M.O. Bodunrin, A.A. Awe, Microstructure, mechanical and fracture properties of groundnut shell ash and silicon carbide dispersion strengthened aluminium matrix composites, *J. Saud. Univ. Eng. Sci.*, 30, 1, 2018, 96-103. <https://doi.org/10.1016/j.jksues.2016.01.001>
4. J.B. Ferguson, H.F. Lopez, P.K. Rohatgi, K. Cho, C.S. Kim, Impact of volume fraction and size of reinforcement particles on the grain size in metal-matrix micro and nanocomposites, *Metall. Mater. Trans. A*, 45, 2014, 4055-4061.
5. B.E. Arendarchuck, L.A. Lourençato, H.D.C. Fals, A.R. Mayer, C.R.C. Lima, Assessment of the microstructure and abrasive wear properties of an A380/NbC aluminum composite produced by stir casting, *Int. J. Metalcast.*, 2, 2023, 1783-1799. <https://doi.org/10.1007/s40962-023-01154-y>
6. H. Bilgen, O. Sahin, N. Akar, V. Kilicli, Dry sliding wear behavior of AA7075 alloy produced by thixocasting, *Mater. Test.*, 66, 1, 2024, 88-99. <https://doi.org/10.1515/mt-2023-0338>
7. P. Ikubanni, M. Oki, A. Adeleke, O. Adesina, P. Omoniyi, Physico-tribological characteristics and wear mechanism of hybrid reinforced Al6063 matrix composites, *Acta Metall. Slovaca*, 27, 4, 2021, 172-179. <https://doi.org/10.36547/ams.27.4.1084>
8. T. Keerthipalli, A. Biswas, R. Aepuru, Mechanical and tribological behavior of Ti₂AlC reinforced hypereutectic aluminium alloy matrix composite fabricated by vacuum assisted induction melting: experimental and theoretical modelling, *Int. J. Metalcast*, 18, 2024, 1173-1191. <https://doi.org/10.1007/s40962-023-01115-5>
9. G.B.V. Kumar, P. P. Panigrahy, N. Suresh, R. Pramod, C.S.P. Rao, Assessment of mechanical and tribological characteristics of silicon nitride reinforced aluminum metal matrix composites, *Compos. Part B-Eng.*, 175, 15, 2019, 107138. <https://doi.org/ARTN10713810.1016/j.compositesb.2019.107138>
10. R.V. Lantmann, A.M.S. Mariante, T.V. Pinheiro, E.M. Da Costa, C.A. Dos Santos, Microstructure, hardness, and linear reciprocating sliding wear response of directionally solidified Al-(2.5,3.5,4.5) Cu-(0.25,0.50)Cr alloys. *Metals*, 13, 7, 2023, 1178. <https://doi.org/10.3390/met13071178>
11. J. Odusote, A. Adeleke, P.I. Qudus, Q. Badurdeen, S. Adeiza, O. Ogunniyi, T. Ogedengbe, Assessment of tribological properties of stir cast Al6063 alloy reinforced with okaba coal ash. *Acta Metall. Slovaca*, 29, 1, 2023, 39-43. <https://doi.org/10.36547/ams.29.1.1750>
12. P. Sarmah, P.K. Patowari, Mechanical and Tribological Analysis of the Fabricated Al6063-based MMCs with SiC Reinforcement Particles, *Silicon*, 15, 2023, 2781-2796
13. A. Jolokhani, A. Razaghian, A. Moharami, M. Emamy, Microstructure and tribological properties of as-cast and multi-pass friction stir processed Mg-0.5Zn-0.5Zr/SiC composite fabricated by stir casting technique, *J. Mater. Res. Technol.*, 27, 2023, 7823-7838, <https://doi.org/10.1016/j.jmrt.2023.11.205>
14. K.K. Alaneme, A.O. Aluko, Fracture toughness (K_{IC}) and tensile properties of ascast and age-hardened aluminium (6063) - silicon carbide particulate composite, *Sci. Iran-Trans. A: Civil Eng. (Elsevier)*, 19, 2012, 992-996.
15. K.K. Alaneme, I.B. Akintunde, P.A. Olubambi, T.M. Adewale, Fabrication characteristics and mechanical behaviour of rice husk ash - alumina reinforced Al-Mg-Si alloy matrix hybrid composites, *J. Mater. Res. Technol.*, 2, 2013, 60-67.
16. ASTM E 92-82, Standard test method for vickers hardness of metallic materials, West Conshohocken (PA): ASTM International, 2003. www.astm.org
17. R.N. Ibrahim, H.L. Stark, Validity requirements

- for fracture toughness measurements from small circumferential notched cylindrical specimens, *Eng. Fract. Mech.*, 28, 1987, 455-460.
18. G.E. Dieter, *Mechanical metallurgy*, SI Metric, edition. Singapore, McGraw-Hill, 1988.
19. K.K. Alaneme, B.U. Odoni, Mechanical properties, wear and corrosion behaviour of copper matrix composites reinforced with steel machining chips, *Eng. Sci. Technol. Int. J.*, 19, 3, 2016, 1593-1599. <https://doi.org/10.1016/j.jestch.2016.04.006>
20. S. Fu, X. Feng, B. Lauke, Y. Mai, Effects of particle size, particle/matrix interface adhesion and particle loading on mechanical properties of particulate-polymer composites, *Compos. Part B Eng.*, 39, 2008, 933-961.
21. I.O. Oladele, J.L. Olajide, M. Amujede, Wear resistance and mechanical behaviour of epoxy/mollusk shell biocomposites developed for structural applications, *Tribo. Ind.*, 38, 3, 2016, 347-360
22. K.K. Alaneme, K.O. Sanusi, Mechanical and wear behaviour of rice husk ash-alumina-graphite hybrid reinforced aluminium based composites, *Eng. Sci. Technol. Int. J.*, 18, 2015, 416-422.
23. K.K. Alaneme, B.J. Bamike, Characterization of mechanical and wear properties of aluminium based composites reinforced with quarry dust and silicon carbide, *Ain Shams Eng. J.*, 9, 4, 2018, 2815-2821. <https://doi.org/10.1016/j.asej.2017.10.009>
24. K.K. Alaneme, P.A. Olubambi, Corrosion and wear behaviour of rice husk ash alumina reinforced Al-Mg-Si alloy matrix hybrid composites, *J. Mater. Res. Technol.*, 2, 2013, 188-194.

